

On the Spectrum Sensing, Beam Selection and Power Allocation in Cognitive Radio Networks Using Reconfigurable Antennas

Hassan Yazdani, Azadeh Vosoughi, *Senior Member, IEEE*
University of Central Florida

E-mail: h.yazdani@knights.ucf.edu, azadeh@ucf.edu

Abstract—In this paper, we consider a cognitive radio (CR) system consisting of a primary user (PU) and a pair of secondary user transmitter (SU_{tx}) and secondary user receiver (SU_{rx}). The SU_{tx} is equipped with a reconfigurable antenna (RA) which divides the angular space into M sectors. The RA chooses one sector among M sectors for its data transmission to SU_{rx}. The SU_{tx} first senses the channel and monitors the activity of PU for a duration of T_{sen} seconds. We refer to this period as *channel sensing phase*. Depending on the outcome of this phase, SU_{tx} stays in this phase or enters the next phase, which we refer to as *transmission phase*. The transmission phase itself consists of two phases: *channel training phase* followed by *data transmission phase*. During the former phase, SU_{tx} sends pilot symbols to enable channel training and estimation at SU_{rx}. The SU_{rx} selects the best beam (sector) for data transmission and feeds back the index of the selected beam as well as its corresponding channel gain. We also derive the probability of determining the true beam and take into account this probability in our system design. During the latter phase, SU_{tx} sends data symbols to SU_{rx} over the selected beam with constant power Φ if the gain corresponding to the selected beam is bigger than the threshold ζ . We find the optimal channel sensing duration T_{sen} , the optimal power level Φ and a optimal threshold ζ , such that the ergodic capacity of CR system is maximized, subject to average interference and power constraints. In addition, we derive closed form expressions for outage and symbol error probabilities of our CR system.

I. INTRODUCTION

The explosive rise in demand for high data rate wireless applications has turned the spectrum into a scarce resource. Cognitive radio (CR) is a promising solution which alleviates spectrum scarcity problem by allowing an unlicensed or secondary user (SU) to access licensed bands in a such way that its imposed interference on license holder primary users (PUs) is limited [1]–[5].

With the help of directional antennas, a system designer can go beyond just filling the spectrum holes in time and/or frequency domains and can further improve the spectral efficiency (well beyond what is attainable with omni-directional antennas), via utilizing the spectrum white spaces in spatial (angular) domain and allowing a PU and a SU use simultaneously the same frequency band, by steering their directional antenna beams to non-interfering directions. Consider an opportunistic CR network where SUs are equipped with directional antennas. SUs can identify the spectrum holes in spatial (angular) domain and use the identified unused directions for data communication. This significantly enhances

the spectrum utilization, compared to the scenario where SUs in the same network are equipped with omni-directional antennas [6]–[8].

Reconfigurable antennas (RAs), with the capabilities of dynamically modifying their characteristics (e.g., operating frequency, radiation pattern, polarization) are emerging as promising solutions to efficiently utilize the spatial (angular) domain and beam steering in wireless communication systems, including CR networks [9]. RA has been used for identifying the directional spectrum sensing opportunities in CR networks as well as for directional wireless and millimeter wave communication systems and surveillance [10], [11]. An electrically steerable parasitic array radiator (ESPAR) antenna is a special kind of RAs, that has been used for identifying the spectral holes in spatial domain in CR networks. ESPAR divides the angular domain into several sectors (beams) and switches between beampatterns of sectors in a time-division fashion (only one of M beams is active at a time). For CR networks, the RAs can provide an improved spectrum sensing and transmit/receive capability, due to a signal-to-noise ratio (SNR) increase for transmission and reception of directional signals, and can limit out-of-band interference to and from PUs [12]. It has been demonstrated that RAs have the ability to transmit multiple data streams by projecting on beamspace basis [13]. Also, they can be used for blind interference alignment through beampattern switching [14]. RAs have been used for performance enhancement of multiple-input multiple-output (MIMO) systems, via exploiting the additional degree of freedom provided by beam selection and enabling joint beam and antenna selection optimization [15]–[17].

In this paper, we consider a CR system consisting of a PU and a pair of SU transmitter (SU_{tx}) and SU receiver (SU_{rx}). The SU_{tx} is equipped with a reconfigurable antenna with the capability of choosing one sector among M sectors for its data transmission to SU_{rx}. The SU_{tx} first senses the channel and monitors the activity of PU for a duration of T_{sen} seconds. We refer to this period as *channel sensing phase*. Depending on the outcome of this phase, SU_{tx} stays in this phase or enters the next phase, which we refer to as *transmission phase*. The transmission phase itself consists of two phases: *channel training phase* followed by *data transmission phase*. During the former phase, SU_{tx} sends pilot symbols to enable channel training and estimation at SU_{rx}. The SU_{rx} selects the best beam (sector) for data transmission and feeds back the index of the

selected beam as well as its corresponding channel gain. We also derive the probability of determining the true beam and take into account this probability in our system design. During the latter phase, SU_{tx} sends data symbols to SU_{rx} over the selected beam with constant power Φ if the gain corresponding to the selected beam is bigger than a threshold ζ . Our objective is to find the optimal channel sensing duration T_{sen} , the optimal power level Φ and the optimal threshold ζ , such that the ergodic capacity of CR system is maximized, subject to average interference and power constraints. In addition, we derive closed form expressions for outage and symbol error probabilities of our CR system.

II. SYSTEM MODEL

Our CR system model is shown in Fig. 1, consisting of a PU and a pair of SU_{tx} and SU_{rx} . We note that PU in our system model can be a primary transmitter or receiver. Similar to [18], we assume when PU is active it is engaged in a bidirectional communication with another PU. The other PU is located far from SU_{tx} and its activity is not considered in this paper. The SU_{tx} is equipped with a RA (for both channel sensing and communication) with the capability of choosing one sector among M sectors for its data transmission to SU_{rx} , while SU_{tx} and PU use omni-directional antennas¹. Similar to [19], we model the radiation pattern of every sector of SU_{tx} 's antenna in x - y (azimuth) plane, with the Gaussian pattern as

$$p(\phi) = A_1 + A_0 e^{-B \left(\frac{\mathcal{M}(\phi)}{\phi_{3dB}} \right)^2}, \quad (1)$$

where

$$\mathcal{M}(\phi) = \text{mod}_{2\pi}(\phi + \pi) - \pi, \quad (2)$$

$\text{mod}_{2\pi}(\phi)$ denotes the remainder of $\frac{\phi}{2\pi}$, $B = \ln(2)$, ϕ_{3dB} is the half-power beam-width, A_1 and A_0 are two constant antenna parameters. We set $A_1 = LA_0$ where $L \ll 1$ is the antenna loss in side lobe. We denote the radiation pattern of m -th sector in angle ϕ by

$$p_m(\phi) = p(\phi - \kappa_m) \quad (3)$$

where $\kappa_m = \frac{2\pi(m-1)}{M}$. In Fig. 2, the beampatterns of a RA with 8 sectors are shown. The orientation of PU and SU_{rx} with respect to SU_{tx} are denoted by ϕ_{PU} and ϕ_{SR} , respectively, and we assume that SU_{tx} knows ϕ_{SR} . The fading coefficients from PU to SU_{tx} , SU_{tx} to SU_{rx} and PU to SU_{rx} are denoted by h , h_{ss} and h_{sp} , respectively, if SU_{tx} uses omni-directional antenna. We model the fading coefficients as circularly symmetric complex Gaussian random variables, and, $g = |h|^2$, $g_{ss} = |h_{ss}|^2$ and $g_{sp} = |h_{sp}|^2$ are mutually independent exponentially distributed random variables with mean γ , γ_{ss} and γ_{sp} , respectively. In our problem, we assume that SUs and PU cannot cooperate and SUs cannot estimate g and g_{sp} . However, we assume that SU_{tx} knows mean values γ and γ_{sp} . Let ψ_m and χ_m denote the fading coefficients of channel between m -th sector of SU_{tx} and PU, and between m -th sector of SU_{tx} and SU_{rx} , respectively, where $\psi_m = h\sqrt{p_m(\phi_{PU})}$, $\chi_m = h_{ss}\sqrt{p_m(\phi_{SR})}$ and $p_m(\phi_{PU})$ and $p_m(\phi_{SR})$ indicate the radiation pattern of m -th sector at angles

¹Throughout this paper, "sector" and "beam" are used interchangeably.

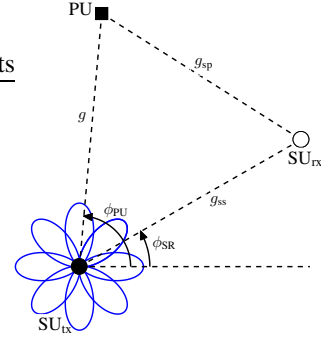


Fig. 1: Our cognitive radio system with reconfigurable antenna.

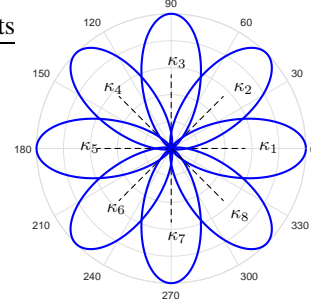


Fig. 2: Beampatterns of a reconfigurable antenna with 8 sectors.

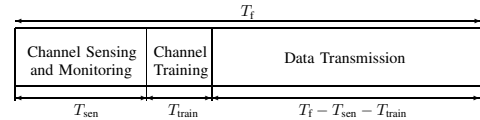


Fig. 3: The structure of frame employed by SU_{tx} .

ϕ_{PU} and ϕ_{SR} , respectively. Also, we assume that the channel gain $\nu_m = |\chi_m|^2$ is an exponential random variable with mean δ_m , and SU_{tx} knows δ_m , for all m [20].

III. OUR PROBLEM STATEMENT

We suppose the SUs employ a frame with a fixed duration of T_f seconds, depicted in Fig. 3. We assume SU_{tx} first senses the channel and monitors the activity of PU. We refer to this period as *channel sensing phase* (with a variable duration of T_{sen} seconds). T_{sen} is the sensing time duration for all M sectors, i.e., every sector senses the channel for T_{sen}/M seconds. Depending on the outcome of this phase, SU_{tx} stays in this phase or enters the next phase, which we refer to as *transmission phase*. The transmission phase itself consists of two phases: *channel training phase* (with a fixed duration of T_{train} seconds) followed by *data transmission phase* (with a variable duration of $T_f - T_{sen} - T_{train}$ seconds). During the former phase, SU_{tx} sends pilot symbols to enable channel training and estimation at SU_{rx} . During the latter phase, SU_{tx} sends data symbols to SU_{rx} . Given T_f and T_{train} we have $0 < T_{sen} < T_f - T_{train}$. In the following, we describe how SU_{tx} operates during these three distinct phases. Based on these descriptions, we provide our problem statement.

A. Channel Sensing Using RA

During this phase, SU_{tx} senses the channel and monitors the activity of PU. Suppose \mathcal{H}_1 and \mathcal{H}_0 represent the binary hypotheses of PU being active and inactive, respectively, with prior probabilities $\Pr\{\mathcal{H}_1\} = \pi_1$ and $\Pr\{\mathcal{H}_0\} = \pi_0$. SU_{tx} applies a binary detection rule to decide whether or not PU is active. Let $\hat{\mathcal{H}}_1$ and $\hat{\mathcal{H}}_0$ denote the detector outcome. When active, PU transmits signal $s(t)$ with power P_p . We assume SU_{tx} collects $N = \lfloor T_{\text{sen}}/(MT_s) \rfloor$ samples at each sector, where T_s is the sampling period. We denote the discrete-time symbol received in m -th sector of SU_{tx} at time instant $t = nT_s$ as

$$y_m(n) = \psi_m(n)s(n) + w_m(n),$$

We model the transmitted signal $s(n)$ by PU as $s(n) \sim \mathcal{CN}(0, P_p)$. The term $w_m(n)$ is the additive noise at m -th sector of SU_{tx}'s antenna and is modeled as $w_m(n) \sim \mathcal{CN}(0, \sigma_w^2)$. It is assumed that $\psi_m(n), w_m(n)$ and $s(n)$ are mutually independent. We assume $w_m(n)$ are independent and thus uncorrelated in both time and space domains, i.e., $\mathbb{E}\{w_m(i)w_{m'}^*(i')\} = \sigma_w^2 \delta[m - m'] \delta[i - i']$ where $\delta[\cdot]$ is Kronecker's delta. Since only one beam is active at a time, the channel gains $\psi_m(n)$ are uncorrelated in both time and space domains, i.e., $\mathbb{E}\{\psi(n)\psi^*(n')\} = E_A \gamma \delta[m - m'] \delta[n - n']$, where $E_A = \frac{1}{2\pi} \int_0^{2\pi} p(\theta) d\theta$. The hypothesis testing problem at n -th time instant for m -th sector is then given by

$$\begin{cases} \mathcal{H}_0 : & y_m(n) = w_m(n), \\ \mathcal{H}_1 : & y_m(n) = \psi_m(n)s(n) + w_m(n). \end{cases}$$

Suppose SU_{tx} uses an energy detector to detect the activity of PU and let ε_m be the energy of received signal at sector m . We have

$$\varepsilon_m = \frac{1}{N} \sum_{n=1}^N |y_m(n)|^2. \quad (4)$$

We consider the summation of energies of received signals over all sectors as the decision statistics as:

$$T = \frac{1}{M} \sum_{m=1}^M \varepsilon_m \underset{\mathcal{H}_0}{\overset{\mathcal{H}_1}{\gtrless}} \eta. \quad (5)$$

Under hypothesis \mathcal{H}_0 , for large N we invoke the central limit theorem (CLT), to approximate T as Gaussian with distribution $T \sim \mathcal{N}(\sigma_w^2, \sigma_{T|\mathcal{H}_0}^2)$, where

$$\sigma_{T|\mathcal{H}_0}^2 = \frac{\sigma_w^4}{MN}.$$

Similarly, under hypothesis \mathcal{H}_1 for large N , T can be approximated with another Gaussian with the distribution $T \sim \mathcal{N}(\mu, \sigma_{T|\mathcal{H}_1}^2)$ where $\mu = P_p \gamma E_A + \sigma_w^2$ and

$$\begin{aligned} \sigma_{T|\mathcal{H}_1}^2 &= \frac{1}{MN} \left[\sigma_w^4 + 2\gamma P_p E_A \sigma_w^2 + \gamma^2 P_p^2 (3E_B - MNE_A^2) \right] \\ &\quad + \frac{\gamma^2 P_p^2}{M^2} \sum_{m=1}^M \sum_{m'=1}^M E_{mm'}, \end{aligned}$$

and $E_{mm'} = \frac{1}{2\pi} \int_0^{2\pi} p_m(\theta) p_{m'}(\theta) d\theta$ and $E_B = E_{mm}$. Then, the false alarm and detection probabilities of this energy

detector are given as follows

$$P_{\text{fa}} = Q\left(\frac{\eta - \sigma_w^2}{\sigma_{T|\mathcal{H}_0}}\right), \quad P_{\text{d}} = Q\left(\frac{\eta - \mu}{\sigma_{T|\mathcal{H}_1}}\right).$$

For a given value of $P_{\text{d}} = \bar{P}_{\text{d}}$, the probability of false alarm can be written as

$$P_{\text{fa}} = Q\left(\frac{\sigma_{T|\mathcal{H}_1} Q^{-1}(\bar{P}_{\text{d}}) + \mu - \sigma_w^2}{\sigma_{T|\mathcal{H}_0}}\right). \quad (6)$$

where $Q(\cdot)$ is the Q-function. Therefore, the probabilities of events $\hat{\mathcal{H}}_0$ and $\hat{\mathcal{H}}_1$ become $\hat{\pi}_0 = \Pr\{\hat{\mathcal{H}}_0\} = \pi_1(1 - \bar{P}_{\text{d}}) + \pi_0(1 - P_{\text{fa}})$ and $\hat{\pi}_1 = \Pr\{\hat{\mathcal{H}}_1\} = \pi_1 \bar{P}_{\text{d}} + \pi_0 P_{\text{fa}}$, respectively. The accuracy of channel sensing impacts the maximum information rate that SU_{tx} can transmit reliably to SU_{rx}. Our problem formulation incorporates the effect of imperfect channel sensing on the constrained ergodic capacity maximization.

B. Estimating the orientation of PU (ϕ_{PU})

As long as the channel is sensed busy, SU_{tx} stays in *channel sensing phase*. While being in this phase, SU_{tx} estimates the location (orientation) of PU using one of the methods explained in [19], [21]–[24]. SU_{tx} uses ϕ_{PU} for adapting its transmit power during *data transmission phase*. We note that, there is a non-zero error when SU_{tx} estimates ϕ_{PU} and we can incorporate this error in our system design and performance analysis. However, in this paper we assume that SU_{tx} can estimate ϕ_{PU} perfectly (with no error).

C. Determining the Sector Corresponding to SU_{rx} and Finding the Strongest Channel between SU_{tx}-SU_{rx}

When the channel is sensed idle, SU_{tx} leaves *channel sensing phase* and enters *channel training phase*. Suppose SU_{tx} knows SU_{rx} is located between two adjacent sectors, however, it does not know which one is better, in terms of enabling a higher transmission rate. During channel training phase, SU_{tx} sends pilot symbols over these two sectors, to enable channel training and estimation at SU_{rx}. Without loss of generality, suppose SU_{rx} is located between the first and second sectors as shown in Fig. 4a. Using the received training signal, SU_{rx} estimates the channel gains $\nu_m = |\chi_m|^2$, $m = 1, 2$ and determines the strongest channel $\nu^* = \max\{\nu_1, \nu_2\}$ and the corresponding beam index $m_{\text{SR}}^* = \arg \max\{\nu_1, \nu_2\}$. For example in Fig. 4b, we have $m_{\text{SR}}^* = 2$, i.e., the second beam has the strongest channel gain. Then, SU_{rx} feeds back m_{SR}^* as well as the value of ν^* to SU_{tx}. We take into account the probability of determining the true sector corresponding to SU_{rx} on the constrained capacity maximization.

We denote the correlation coefficient between channel gains of sectors m and m' by $\rho_{mm'}$. The correlation coefficient depends on the structure and design of RA [16] and we assume SU_{tx} has complete knowledge of the correlation coefficient $\rho_{mm'}$. Let ρ represent the correlation coefficient between two adjacent sectors which SU_{rx} is located. The joint probability distribution function (PDF) and cumulative density function (CDF) of channel gains ν_1 and ν_2 can be written as following

$$f_{\nu_1 \nu_2}(y_1, y_2) = \frac{\alpha_1}{\delta_2} e^{-\alpha_1 y_1} e^{-\alpha_2 y_2} I_0\left(2\sqrt{\rho^2 \alpha_1 \alpha_2 y_1 y_2}\right) \quad (7)$$

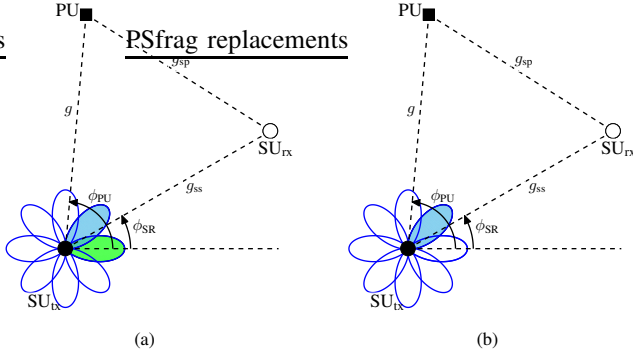


Fig. 4: A schematic to show how SU_{tx} selects the strongest channel between SU_{tx} and SU_{rx} (a) SU_{rx} is located between the first and second beams (sectors), (b) The second sector is selected for data transmission ($m_{SR}^* = 2$).

$$F_{\nu_1\nu_2}(y_1, y_2) = 1 - e^{-\frac{y_1}{\delta_1}} Q_1\left(\sqrt{2\alpha_2 y_2}, \sqrt{2\rho^2 \alpha_1 y_1}\right) - e^{-\frac{y_2}{\delta_2}} \left[1 - Q_1\left(\sqrt{2\rho^2 \alpha_2 y_2}, \sqrt{2\alpha_1 y_1}\right)\right] \quad (8)$$

where $\alpha_m = \frac{1}{\delta_m(1-\rho^2)}$ for $m = 1, 2$, $I_0(\cdot)$ is the modified Bessel function of the first kind and $Q_1(\cdot, \cdot)$ is the Marcum Q-function. Then the CDF of selected gain ν^* is $F_{\nu^*}(x) = F_{\nu_1\nu_2}(x, x)$ and the PDF is

$$f_{\nu^*}(x) = \frac{1}{\delta_1} e^{-\frac{x}{\delta_1}} \left[1 - Q_1\left(\sqrt{2\rho^2 \alpha_1 x}, \sqrt{2\alpha_2 x}\right)\right] + \frac{1}{\delta_2} e^{-\frac{x}{\delta_2}} \left[1 - Q_1\left(\sqrt{2\rho^2 \alpha_2 x}, \sqrt{2\alpha_1 x}\right)\right]. \quad (9)$$

The probability of the first beam being selected when SU_{rx} is between the first and second beams becomes

$$\Delta_1 = \Pr\{m_{SR}^* = 1\} = \Pr(\nu_1 > \nu_2) = \int_0^\infty \int_0^x f_{\nu_1, \nu_2}(x, y) dy dx = \frac{1}{\alpha_2 \delta_2} \sum_{k=0}^\infty \rho^{2k} \left[1 - \left(\frac{\alpha_1}{\alpha_2}\right)^{k+1} \times \frac{\Gamma(2k+2)}{(k+1)(k!)^2} {}_2F_1\left(k+1, 2(k+1); k+2; \frac{-\alpha_1}{\alpha_2}\right)\right] \quad (10)$$

where ${}_2F_1(\cdot, \cdot; \cdot; \cdot)$ is the hypergeometric function [25]. In special case when $\rho = 0$, we have $\Delta_1 = \frac{\delta_1}{\delta_1 + \delta_2}$.

D. Data Transmission

When the channel is sensed idle, SU_{tx} sends data to SU_{rx} over the selected sector (m_{SR}^*) using the following power control policy

$$P(\nu^*) = \begin{cases} \Phi, & \text{if } \nu^* \geq \zeta \\ 0, & \text{if } \nu^* < \zeta \end{cases} \quad (11)$$

According to (11), when the selected channel (sector) is too weak (ν^* is less than the cut-off threshold ζ) SU_{tx} does not transmit data. However, when channel is strong enough, SU_{tx} sends data with constant power Φ . We find Φ and ζ such that the ergodic capacity of SU_{tx}-SU_{rx} link is maximized. The ergodic capacity of SU_{tx}-SU_{rx} link is [8]

$$C = D_t \mathbb{E}\{\alpha_0 c_{0,0} + \beta_0 c_{1,0}\}, \quad (12)$$

where $D_t = (T_f - T_{sen} - T_{train})/T_f$ is the fraction of time in which SU_{tx} sends data to SU_{rx}, $c_{i,0}$ is the instantaneous capacity of this link corresponding to the event \mathcal{H}_i and $\hat{\mathcal{H}}_0$, given as

$$c_{0,0} = \log_2 \left(1 + \frac{\nu^* P(\nu^*)}{\sigma_w^2}\right), \quad (13)$$

$$c_{1,0} = \log_2 \left(1 + \frac{\nu^* P(\nu^*)}{\sigma_w^2 + P_p g_{sp}}\right), \quad (14)$$

and $\alpha_0 = \pi_0(1 - P_{fa})$, $\beta_0 = \pi_1(1 - \bar{P}_d)$. Let \bar{I}_{av} indicate the maximum allowed interference power imposed on PU and \bar{P}_{av} denote the maximum allowed average transmit power of SU_{tx}. To satisfy the average interference constraint (AIC), we have

$$D_t \beta_0 \mathbb{E}\{g_{sp} p(\kappa_{SR}^* - \phi_{PU}) P(\nu^*)\} \leq \bar{I}_{av}, \quad (15)$$

and to satisfy the average power constraint (APC), we have

$$D_t \hat{\pi}_0 \mathbb{E}\{P(\nu^*)\} \leq \bar{P}_{av}. \quad (16)$$

Notice that for a given T_f , if we increase the sensing time T_{sen} , the spectrum sensing will be more accurate and data communication between SU_{tx} and SU_{rx} would cause less interference on PU. On the other hand, the available time for data transmission to SU_{rx} decreases. Therefore, a trade-off exists between sensing and transmission capacity in terms of T_{sen} . Our main objective is to find the optimal channel sensing duration T_{sen} , the optimal power level Φ and the optimal threshold ζ , such that the ergodic capacity C in (12) is maximized, subject to AIC and APC given in (15) and (16), respectively. In other words, we are interested in solving the following constrained optimization problem

$$\text{Maximize } C = D_t \mathbb{E}\{\alpha_0 C_{0,0} + \beta_0 C_{1,0}\} \quad (P1)$$

T_{sen}, Φ, ζ

$$\text{s.t.} \quad 0 < T_{sen} < T_f - T_{train},$$

$$\Phi \geq 0, \zeta \geq 0,$$

(15) and (16) are satisfied.

IV. FORMALIZING AND SOLVING (P1)

Since SUs and PU cannot cooperate, SU_{tx} cannot estimate the channel gain g_{sp} and thus $c_{1,0}$ cannot be directly maximized at SU_{tx}. Instead, we consider a lower bound on its average over g_{sp} , denoted as $\mathbb{E}_{g_{sp}}\{c_{1,0}\}$. Using the Jensen's inequality [26], the lower bound on $\mathbb{E}_{g_{sp}}\{c_{1,0}\}$ becomes

$$\mathbb{E}_{g_{sp}}\{c_{1,0}\} \geq \log_2 \left(1 + \frac{\nu^* P(\nu^*)}{\sigma_w^2 + \sigma_p^2}\right) = c_{1,0}^{LB} \quad (17)$$

where $\sigma_p^2 = P_p \gamma_{sp}$. Let $C^{LB} = D_t \mathbb{E}_{\nu^*}\{\alpha_0 c_{0,0} + \beta_0 c_{1,0}^{LB}\}$ where C^{LB} is the lower bound on C in (12). From now on, we focus on C^{LB} . Next, we focus on the AIC in (15) and find the term $\mathbb{E}\{p(\kappa_{SR}^* - \phi_{PU})\}$. By using the average probabilities derived in (10) we have

$$\mathbb{E}\{p(\kappa_{SR}^* - \phi_{PU})\} = \Delta_1 p(\kappa_1 - \phi_{PU}) + \Delta_2 p(\kappa_2 - \phi_{PU}).$$

$$C_{\text{Opt}}^{\text{LB}} = \max_{\zeta, T_{\text{sen}}} \frac{D_t}{\ln(2)} \left[\sum_{m=1}^2 \left[\alpha_0 G(\delta_m, \text{SNR}^{(0)}, \zeta) + \beta_0 G(\delta_m, \text{SNR}^{(1)}, \zeta) \right] - \sum_{j=0}^{\infty} \sum_{i=0}^j D_{ij} \left[\alpha_0 V(i+j, \omega, \text{SNR}^{(0)}, \zeta) + \beta_0 V(i+j, \omega, \text{SNR}^{(1)}, \zeta) \right] \right] \quad (20)$$

$$V(n, \omega, \mathbf{S}, \zeta) = \frac{n}{\omega} V(n-1, \omega, \mathbf{S}, \zeta) + \frac{\zeta^n}{\omega} G(1/\omega, \mathbf{S}, \zeta) + \frac{n}{\omega} e^{\frac{\omega}{\mathbf{S}}} H(n-1, \omega, \mathbf{S}, \zeta) \quad (21a)$$

$$H(k, \omega, \mathbf{S}, \zeta) = \sum_{j=0}^k \binom{k}{j} \frac{(-\mathbf{S})^{j-k}}{(j+1) \omega^{j+1}} \left[\left(\omega \zeta + \frac{\omega}{\mathbf{S}} \right)^{j+1} \text{Ei} \left(-\omega \zeta - \frac{\omega}{\mathbf{S}} \right) + \Gamma \left(j+1, \omega \zeta + \frac{\omega}{\mathbf{S}} \right) \right] \quad (21b)$$

By defining $b_0 = \beta_0 \gamma_{\text{sp}} [\Delta_1 p(\kappa_1 - \phi_{\text{PU}}) + \Delta_2 p(\kappa_2 - \phi_{\text{PU}})]$, the optimal power Φ , given T_{sen} and ζ can be easily obtained as

$$\Phi = \frac{1}{(1 - F_{\nu^*}(\zeta))} \min \left\{ \frac{\bar{P}_{\text{av}}}{D_t \hat{\pi}_0}, \frac{\bar{I}_{\text{av}}}{D_t b_0} \right\}. \quad (18)$$

To obtain a closed form for ergodic capacity, we expand the PDF in (9) using the following equation

$$Q_1(\sqrt{\lambda}, \sqrt{y}) = \sum_{j=0}^{\infty} \frac{(\frac{\lambda}{2})^j}{j!} e^{-\frac{(y+\lambda)}{2}} \sum_{i=0}^j \frac{(\frac{y}{2})^i}{i!}.$$

and rewrite $f_{\nu^*}(x)$ as the following form

$$f_{\nu^*}(x) = \sum_{m=1}^2 \frac{1}{\delta_m} e^{-\frac{x}{\delta_m}} - \sum_{j=0}^{\infty} \sum_{i=0}^j D_{ij} x^{i+j} e^{-x\omega} \quad (19)$$

where $\omega = \alpha_1 + \alpha_2$ and $D_{ij} = \frac{\rho^{2j}}{j! i!} \left(\frac{\alpha_1^j \alpha_2^i}{\delta_1} + \frac{\alpha_1^i \alpha_2^j}{\delta_2} \right)$. To solve (P1), we consider two initial values for ζ and T_{sen} and obtain Φ using (18). Then, ζ^{opt} and $T_{\text{sen}}^{\text{opt}}$ can be obtained by maximizing the ergodic capacity given in (20) using searching methods such as bisection, where

$$\text{SNR}^{(0)} = \frac{\Phi}{\sigma_w^2}, \quad \text{SNR}^{(1)} = \frac{\Phi}{\sigma_w^2 + \sigma_p^2},$$

$$G(\delta, \mathbf{S}, \zeta) = e^{-\frac{\zeta}{\delta}} \ln(1 + \mathbf{S}\zeta) - e^{\frac{1}{\delta \mathbf{S}}} \text{Ei} \left(\frac{-1}{\delta \mathbf{S}} (1 + \mathbf{S}\zeta) \right),$$

and $\text{Ei}(\cdot)$ is the exponential integral [25] and $V(\cdot)$ can be calculated using the recursive equation in (21). In (21b), $\Gamma(\cdot, \cdot)$ is the incomplete Gamma function.

V. OUTAGE AND SYMBOL ERROR PROBABILITIES

Two other relevant metrics to evaluate the performance of our CR system with the RA at SU_{tx} are outage probability and symbol error probability (SEP), denoted as P_{out} and P_e , respectively. We define P_{out} as the probability of SU_{tx} not transmitting data due to the weak $\text{SU}_{\text{tx}}\text{-SU}_{\text{rx}}$ channel. In the following, we derive closed-form expressions for P_{out} and P_e . The outage probability P_{out} can be directly obtained using the CDF of ν^* as

$$P_{\text{out}} = \Pr \{P(\nu^*) = 0\} = F_{\nu^*}(\zeta). \quad (22)$$

For many digital modulation schemes SEP can be written as a function with the following form [17]

$$P_e = \mathbb{E} \left\{ Q(\sqrt{\Psi \text{SNR}_{\text{rx}}}) \right\}, \quad (23)$$

where Ψ is a constant parameter related to the type of modulation and SNR_{rx} is the received signal-to-noise-ratio (SNR) at SU_{rx} given as

$$\text{SNR}_{\text{rx}} = \begin{cases} \frac{\Phi \nu^*}{\sigma_w^2}, & \text{if } \nu^* \geq \zeta, (\mathcal{H}_0, \hat{\mathcal{H}}_0) \\ \frac{\Phi \nu^*}{\sigma_w^2 + \sigma_p^2}, & \text{if } \nu^* \geq \zeta, (\mathcal{H}_1, \hat{\mathcal{H}}_0) \\ 0, & \text{else} \end{cases} \quad (24)$$

After some manipulation, SEP can be written as (25), where

$$J(k, \mathbf{S}, \Psi, \omega, \zeta) = \frac{1}{\mathbf{S}^k} \left(\frac{\omega}{\mathbf{S}\Psi} + \frac{1}{2} \right)^{-k-\frac{1}{2}} \Gamma \left(k + \frac{1}{2}, \left(\frac{\mathbf{S}\Psi}{2} + \omega \right) \zeta \right)$$

$$\text{and } E_{ij} = \frac{\alpha_1^i \alpha_2^j}{i! j!} (\rho^{2j} - \rho^{2i}).$$

VI. SIMULATION RESULTS

In this section, we illustrate the effect of reconfigurable antennas on the ergodic capacity and outage and symbol error probabilities of our secondary network by Matlab simulations. Assume $\sigma_w^2 = 1$, $\gamma_{\text{ss}} = \gamma_{\text{sp}} = \gamma = 1$, $\pi_1 = 0.4$, $L = 0.01$, $T_f = 10$ ms, $f_s = 100$ KHz, $\bar{P}_d = 0.85$, $P_p = 0.2$ watts, $\Psi = 4$.

When beam-width of sectors increases, RA spreads electromagnetic power in a wider area. To fairly compare the performance of our system with different $\phi_{3\text{dB}}$, we choose A_0 such that $E_A = 1$. The beampatterns of a sector of RA for $\phi_{3\text{dB}} = 25^\circ, 35^\circ$ and the beampattern of a traditional omnidirectional antenna are shown in Fig. 5a. We can see that by decreasing $\phi_{3\text{dB}}$ and setting $E_A = 1$, the gain of antenna in 0° increases. Fig. 5b shows the probability of detection versus the probability of false alarm for $N = 16$, $M = 8$ and $\phi_{3\text{dB}} = 20^\circ, 25^\circ, 30^\circ$. We observe that as $\phi_{3\text{dB}}$ increases, P_d increases.

The probability of first beam selection (Δ_1) versus $\phi_{3\text{dB}}$ is plotted in Fig. 6 for $M = 8$ when SU_{rx} is located at $\phi_{\text{SR}} = 0^\circ, 10^\circ, 15^\circ$. If we increase the beam-width $\phi_{3\text{dB}}$, Δ_1 decreases, i.e., to increase Δ_1 , we need a narrower beam-width. Also, we note that when ϕ_{SR} approaches 0° , the beam selection is more accurate.

$$P_e = \frac{1}{2\sqrt{2\pi}} \left[\left[\alpha_0 J(0, \text{SNR}^{(0)}, \Psi, 0, \zeta) + \beta_0 J(0, \text{SNR}^{(1)}, \Psi, 0, \zeta) \right] \left(1 - F_{\nu^*}(\zeta) \right) - \alpha_0 J\left(0, \text{SNR}^{(0)}, \Psi, \frac{1}{\delta_2}, \zeta\right) - \beta_0 J\left(0, \text{SNR}^{(1)}, \Psi, \frac{1}{\delta_2}, \zeta\right) \sum_{j=0}^{\infty} \sum_{i=0}^j \frac{E_{ij}}{\Psi^{i+j}} \left(\alpha_0 J(i+j, \text{SNR}^{(0)}, \Psi, \omega, \zeta) + \beta_0 J(i+j, \text{SNR}^{(1)}, \Psi, \omega, \zeta) \right) \right] \quad (25)$$

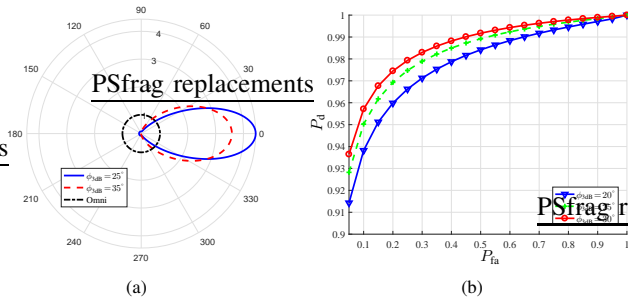


Fig. 5: (a) Beampattern in polar coordination, (b) P_d versus P_{fa} for $\phi_{3dB} = 20^\circ, 25^\circ, 30^\circ$.

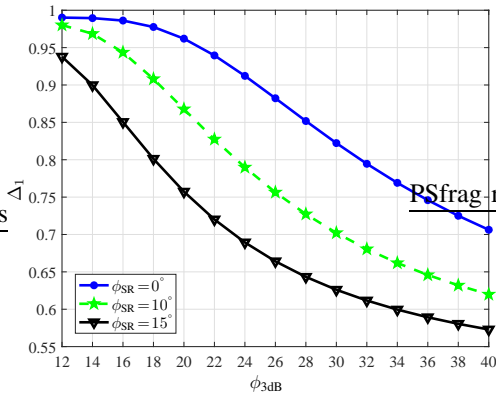


Fig. 6: Δ_1 versus ϕ_{3dB} .

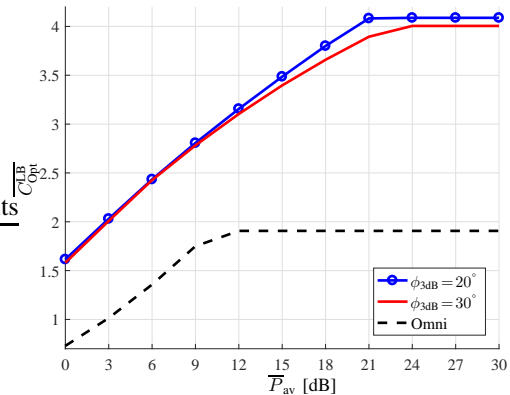


Fig. 7: Optimal Capacity averaged over orientation of SU_{tx} and PU versus \overline{P}_{av} .

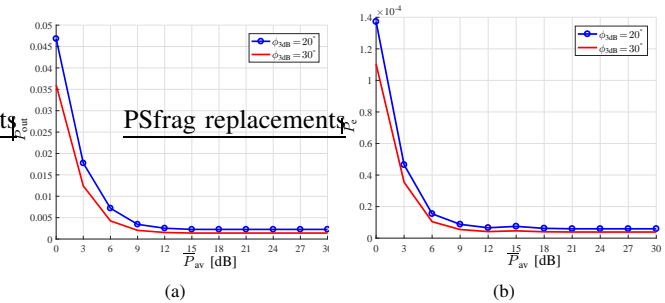


Fig. 8: (a) P_{out} versus \overline{P}_{av} , (b) P_e versus \overline{P}_{av} .

Assume \overline{C}_{Opt}^{LB} is the maximized capacity averaged over all possible orientations of SU_{tx} (ϕ_{SR}) and PU (ϕ_{PU}). Fig. 7 illustrates \overline{C}_{Opt}^{LB} versus \overline{P}_{av} when $M = 8, \overline{I}_{av} = 0$ dB, $\phi_{3dB} = 20^\circ, 30^\circ$. For comparison, the maximized capacity when SU_{tx} equipped with omni-directional antenna and Φ, ζ and T_{sen} are optimized, is plotted. We can see that, in average, RA yields a higher capacity compared to omni-directional antenna. Also, a RA with smaller ϕ_{3dB} yields a higher capacity, because it can cancel more interference imposed on PU from SU_{tx} .

The averaged outage and symbol error probabilities over ϕ_{SR} and ϕ_{PU} (denoted as \overline{P}_{out} and \overline{P}_e) are shown in Figs. 8a and 8b, respectively. Regarding the maximized capacity shown in Fig. 7, we observe that increasing the beam-width from 20° to 30° yields lower outage and symbol error probabilities. However, the other performance metric, i.e. the ergodic capacity, decreases.

VII. CONCLUSION

We considered a CR system consisting of a PU and a pair of SU_{tx} and SU_{rx} . The SU_{tx} is equipped with a RA

which divides the angular space into M sectors. The SU_{tx} first senses the activity of PU and transmits data to SU_{rx} (if the channel is sensed idle) over the strongest channel (sector) of the RA. We obtained the optimal channel sensing duration, the optimal power level and the optimal threshold, such that the ergodic capacity of CR system is maximized, subject to average interference and power constraints. In addition, we derived closed form expressions for outage and symbol error probabilities of our CR system.

ACKNOWLEDGMENT

This research is supported by NSF under grant ECCS-1443942.

REFERENCES

- [1] T. Yucek and H. Arslan, "A survey of spectrum sensing algorithms for cognitive radio applications," *IEEE Communications Surveys Tutorials*, vol. 11, no. 1, pp. 116–130, First 2009.
- [2] H. Zhang, Y. Nie, J. Cheng, V. C. M. Leung, and A. Nallanathan, "Sensing time optimization and power control for energy efficient cognitive small cell with imperfect hybrid spectrum sensing," *IEEE Transactions on Wireless Communications*, vol. 16, no. 2, pp. 730–743, Feb 2017.

- [3] H. Hu, H. Zhang, and Y. C. Liang, "On the spectrum- and energy-efficiency tradeoff in cognitive radio networks," *IEEE Transactions on Communications*, vol. 64, no. 2, pp. 490–501, Feb 2016.
- [4] G. Ozcan, M. C. Gursoy, N. Tran, and J. Tang, "Energy-efficient power allocation in cognitive radio systems with imperfect spectrum sensing," *IEEE Journal on Selected Areas in Communications*, vol. 34, no. 12, pp. 3466–3481, Dec 2016.
- [5] P. Paysarvi-Hoseini and N. C. Beaulieu, "Optimal wideband spectrum sensing framework for cognitive radio systems," *IEEE Transactions on Signal Processing*, vol. 59, no. 3, pp. 1170–1182, March 2011.
- [6] H. Yazdani and A. Vosoughi, "On cognitive radio systems with directional antennas and imperfect spectrum sensing," in *2017 IEEE International Conference on Acoustics, Speech and Signal Processing (ICASSP)*, March 2017, pp. 3589–3593.
- [7] H. Yazdani and A. Vosoughi, "On the combined effect of directional antennas and imperfect spectrum sensing upon ergodic capacity of cognitive radio systems," in *2017 51st Asilomar Conference on Signals, Systems, and Computers*, Oct 2017, pp. 1702–1706.
- [8] H. Yazdani and A. Vosoughi, "On optimal sensing and capacity trade-off in cognitive radio systems with directional antennas," *ArXiv e-prints*, Oct 2018. [Online]. Available: <https://arxiv.org/abs/1810.08251>
- [9] M. Shirazi, T. Li, J. Huang, and X. Gong, "A reconfigurable dual-polarization slot-ring antenna element with wide bandwidth for array applications," *IEEE Transactions on Antennas and Propagation*, vol. 66, no. 11, pp. 5943–5954, Nov 2018.
- [10] M. A. Almasi, R. Amiri, and H. Mehrpouyan, "A new millimeter wave MIMO system for 5G networks," *CoRR*, vol. abs/1807.04851, 2018. [Online]. Available: <http://arxiv.org/abs/1807.04851>
- [11] M. A. Almasi, H. Mehrpouyan, V. Vakilian, N. Behdad, and H. Jafarkhani, "A new reconfigurable antenna MIMO architecture for mmWave communication," in *2018 IEEE International Conference on Communications (ICC)*, May 2018, pp. 1–7.
- [12] D. Wilcox, E. Tsakalaki, A. Kortun, T. Ratnarajah, C. B. Papadias, and M. Sellathurai, "On spatial domain cognitive radio using single-radio parasitic antenna arrays," *IEEE Journal on Selected Areas in Communications*, vol. 31, no. 3, pp. 571–580, March 2013.
- [13] A. M. Alaa, M. H. Ismail, and H. Tawfik, "Random aerial beamforming for underlay cognitive radio with exposed secondary users," *IEEE Transactions on Vehicular Technology*, vol. 65, no. 7, pp. 5364–5383, July 2016.
- [14] R. Qian and M. Sellathurai, "On the implementation of blind interference alignment with single-radio parasitic antennas," *IEEE Transactions on Vehicular Technology*, vol. 65, no. 12, pp. 10 180–10 184, Dec 2016.
- [15] Z. Boudia, H. El-Sallabi, A. Ghayeb, and K. A. Qaraqe, "Reconfigurable antenna-based space-shift keying (SSK) for MIMO Rician channels," *IEEE Transactions on Wireless Communications*, vol. 15, no. 1, pp. 446–457, Jan 2016.
- [16] Z. Boudia, H. El-Sallabi, M. Abdallah, A. Ghayeb, and K. A. Qaraqe, "Reconfigurable antenna-based space-shift keying for spectrum sharing systems under Rician fading," *IEEE Transactions on Communications*, vol. 64, no. 9, pp. 3970–3980, Sept 2016.
- [17] R. Senanayake, P. J. Smith, P. A. Martin, and J. S. Evans, "Performance analysis of reconfigurable antenna arrays," *IEEE Transactions on Communications*, vol. 65, no. 6, pp. 2726–2739, June 2017.
- [18] J. Mansukhani, P. Ray, and P. K. Varshney, "Coupled detection and estimation based censored spectrum sharing in cognitive radio networks," *IEEE Transactions on Wireless Communications*, vol. 15, no. 6, pp. 4206–4217, June 2016.
- [19] J. Werner, J. Wang, A. Hakkarainen, D. Cabric, and M. Valkama, "Performance and Cramér–Rao bounds for DoA/RSS estimation and transmitter localization using sectorized antennas," *IEEE Transactions on Vehicular Technology*, vol. 65, no. 5, pp. 3255–3270, May 2016.
- [20] M. H. Yilmaz, M. M. Abdallah, H. M. El-Sallabi, J. F. Chamberland, K. A. Qaraqe, and H. Arslan, "Joint subcarrier and antenna state selection for cognitive heterogeneous networks with reconfigurable antennas," *IEEE Transactions on Communications*, vol. 63, no. 11, pp. 4015–4025, Nov 2015.
- [21] R. Qian, M. Sellathurai, and T. Ratnarajah, "Directional spectrum sensing for cognitive radio using ESPAR arrays with a single RF chain," in *2014 European Conference on Networks and Communications (EuCNC)*, June 2014, pp. 1–5.
- [22] H. Yazdani, A. Vosoughi, and N. Rahnavard, "Compressive sensing based direction-of-arrival estimation using reweighted greedy block coordinate descent algorithm for ESPAR antennas," in *MILCOM 2017 - 2017 IEEE Military Communications Conference (MILCOM)*, Oct 2017, pp. 169–173.
- [23] A. Jabalameli and A. Behal, "A constrained linear approach to identify a multi-timescale adaptive threshold neuronal model," in *2015 IEEE 5th International Conference on Computational Advances in Bio and Medical Sciences (ICCABS)*, Oct 2015, pp. 1–6.
- [24] J. Wang, J. Werner, M. Valkama, and D. Cabric, "Performance analysis of primary user RSS/DoA estimation and localization in cognitive radio networks using sectorized antennas," *IEEE Wireless Communications Letters*, vol. 3, no. 2, pp. 237–240, April 2014.
- [25] I. S. Gradshteyn and I. M. Ryzhik, *Table of integrals, series, and products*, 2014.
- [26] T. M. Cover and J. A. Thomas, *Elements of Information Theory (Wiley Series in Telecommunications and Signal Processing)*. New York, NY, USA: Wiley-Interscience, 2006.